

## Electronic structure of $\text{Na}_x\text{WO}_3$ : A photoemission study covering the entire concentration range

H. Höchst and R. D. Bringans,\*

*Max-Planck-Institut für Festkörperforschung, Heisenbergstrasse 1,  
7000 Stuttgart 80, Federal Republic of Germany*

H. R. Shanks

*Ames Laboratory, Ames, Iowa 50011*

(Received 22 March 1982)

Angle-resolved and angle-integrated ultraviolet-photoemission-spectroscopy (UPS) investigations have been carried out over the entire concentration range  $0 < x < 1$  of the sodium-tungsten-bronze system  $\text{Na}_x\text{WO}_3$ . The results indicate that the rigid-band model used by several authors fails to explain the  $x$  dependence of the electronic structure. For the metallic samples with  $x \geq 0.3$ , the top of the valence band and the bottom of the conduction band remain at 3 and 1 eV, respectively, and the width of the occupied part of the conduction band is independent of  $x$ . The peak amplitude at the Fermi level varies linearly with  $x$  and does not follow the predicted dependence. A detailed comparison is made between the experimental results and the band-structure calculation of Kopp *et al.* Both the width of the valence band and the separation between the valence and conduction bands are too small in the calculation. Angle-resolved UPS measurements reveal a peak in the gap region for the metallic samples which disperses from 2.1 eV for  $\vec{k}_{\parallel}=0$  to 1.2 eV for  $\vec{k}_{\parallel}$  along  $\Gamma$ - $M$ . This feature is assigned to a surface state. The failure to detect localized gap states for the semiconducting samples is explained by band bending and a charge depletion layer caused by oxygen acceptor states at the surface. The fact that the work function  $\phi$  decreases linearly with increasing  $x$  indicates that there is no surface depletion of sodium as has been claimed earlier.

### I. INTRODUCTION

The sodium-tungsten bronzes  $\text{Na}_x\text{WO}_3$  can be prepared as well-defined crystals over the entire range of sodium concentrations from  $x=0$  to 1.  $\text{Na}_x\text{WO}_3$  is semiconducting at low values of  $x$ , but for  $x$  greater than about 0.25, the material is metallic. Although the semiconductor-metal transition has been the subject of several recent investigations, there is still no generally accepted mechanism for the effect. Suggestions that the material is nonhomogeneous and consists of isolated conducting and nonconducting regions, and hence that the transition can be described in a percolation model,<sup>1,2</sup> have been criticized by several authors.<sup>3-5</sup> In particular, the single-phase x-ray diffraction patterns obtained for these materials indicate that  $\text{Na}_x\text{WO}_3$  is homogeneous<sup>6</sup> and that the transition is due to a more subtle effect.

To a first approximation the electronic structure of metallic  $\text{Na}_x\text{WO}_3$  can be thought of as a semiconductor formed from  $\text{WO}_3$  with conduction electrons provided by the sodium atoms. Results of

Hall-effect measurements are summarized by Lightsey *et al.*<sup>7</sup> and show that the number of conduction electrons increases with  $x$  for  $x > 0.22$ , the absolute number of electrons being very nearly equal to one per sodium atom. The fact that  $\text{Na}_x\text{WO}_3$  is not a metal for all  $x > 0$  means that in the low- $x$  range the conduction electrons must be localized or in an impurity band split by the correlation energy. On the basis of several earlier experimental results, Mott<sup>4</sup> concluded that the most likely cause of the transition is localization due to the random charges introduced by the  $\text{Na}^+$  ions. A structural phase transition that occurs near the semiconductor-metal transition has complicated the analysis, and the details of the localization mechanism are still not fully understood.

The concentration-dependent valence-band behavior of  $\text{Na}_x\text{WO}_3$  outside the transition region is also of considerable interest, and in this paper we examine the electronic behavior of  $\text{Na}_x\text{WO}_3$  over the whole range of  $x$ . Figure 1 shows the crystal structure of  $\text{Na}_x\text{WO}_3$  in the cubic approximation. This structure, which consists of a cubic

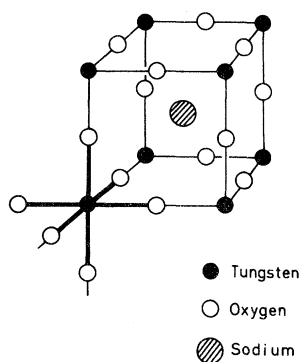


FIG. 1. Structure of  $\text{Na}_x\text{WO}_3$  in the perovskite approximation. The unit cell is cubic and the tungsten atoms are octahedrally surrounded by oxygen atoms. Sodium atoms randomly occupy the position at the cube center at concentrations ranging continuously from 0 to 1 per  $\text{WO}_3$  unit.

$\text{WO}_3$  lattice with sodium atoms randomly occupying the cube body center, is realized in practice only for  $x \gtrsim 0.5$  and at temperatures above about  $160^\circ\text{C}$ .<sup>8</sup> As the sodium concentration decreases, the distortion from the simple cubic structure becomes greater, but the  $\text{WO}_6$  octahedra, or slightly distorted versions of them, remain over the whole range of  $x$ . The simple perovskite structure of Fig. 1 is thus useful for discussing the electronic structure of the metallic phase of  $\text{Na}_x\text{WO}_3$ .

In agreement with experimental NMR studies,<sup>5,7</sup> theoretical band-structure calculations<sup>9</sup> have shown that the conduction electrons in metallic  $\text{Na}_x\text{WO}_3$  are not Na  $s$ -like but occupy a band derived from W  $5d$  and O  $2p$  states. The conduction band of  $\text{WO}_3$  also has the same mixture of W  $5d$  and O  $2p$ , and the similarity has led to an interpretation of the properties of  $\text{Na}_x\text{WO}_3$  using a rigid-band model. In this model, the valence and conduction bands are those from the  $\text{WO}_3$  sublattice, the conduction band simply being "filled" by the extra electron contributed by each sodium atom. Kopp *et al.*<sup>9</sup> calculated the band structures for  $\text{WO}_3$  and  $\text{NaWO}_3$ , with a non-self-consistent Korringa-Kohn-Rostoker (KKR) method, and used the perovskite-structure approximation in both cases. On the basis of the similarity between the bands for the two calculations, Kopp *et al.*<sup>9</sup> concluded that the rigid-band model was a good approximation for  $\text{Na}_x\text{WO}_3$ . This conclusion was reached earlier by Chazalviel *et al.*<sup>10</sup> for values of  $x \geq 0.5$ , based on their x-ray photoelectron spectroscopy (XPS) results and repeated in a recent Communication by Wertheim and Chazalviel.<sup>11</sup>

In a paper describing XPS measurements made

on  $\text{Na}_x\text{WO}_3$  for a wide range of  $x$  values,<sup>12</sup> we criticized the rigid-band interpretation of the earlier XPS measurements. Our argument was that as  $x$  increases, the rigid-band model would require that the occupied part of the conduction-band widths increase by filling electrons into the conduction band. These  $x$ -dependent raisings of the Fermi level should be detectable as an increase in the binding energies of all core levels, as well as an increase in energy between the top of the valence-band relative to the Fermi level. We found, however, that none of these effects occurred.

Wertheim and Chazalviel suggested that the increase in the conduction-band width was within our experimental uncertainty of about 0.1 eV. As we pointed out in Ref. 12, for this possibility to explain the experimental results, a much larger density of states at the bottom of the conduction band than that calculated by Kopp *et al.*<sup>9</sup> would be required. Our XPS results<sup>12</sup> showed that the rigid-band model was invalid for the metallic region of  $\text{Na}_x\text{WO}_3$  and also invalid if attention was restricted only to the cubic region with  $x > 0.50$ . Despite suggestions to the contrary,<sup>11</sup> we did not use the separation between the valence band and the Fermi energy in the semiconducting samples to question the validity of the rigid-band model. The fact that the region of the spectrum near the Fermi energy is strongly affected by oxygen loss for the semiconducting compounds was pointed out<sup>12</sup> and has been examined extensively for the case of  $\text{WO}_3$ .<sup>13</sup>

Further evidence against the rigid-band model is provided by the  $x$  dependence of the electronic specific-heat coefficient and magnetic susceptibility. The summary of data given by Zumsteg<sup>14</sup> shows that both of these quantities vary linearly with  $x$  rather than with the  $x^{1/3}$  behavior expected for a free-electron conduction band, or the behavior expected for a filling of the KKR conduction-band density of states.<sup>9</sup> These results are shown in Fig. 9 and will be discussed later.

To examine these questions about the applicability of the rigid-band model further, and to extend our earlier XPS results, we have carried out ultraviolet photoelectron spectroscopy (UPS) studies of  $\text{Na}_x\text{WO}_3$ . After describing the experimental details in the next section, results of angle-resolved UPS measurements are shown for a vacuum cleaved sample of  $\text{Na}_{0.85}\text{WO}_3$  and compared with the band-structure calculation of Kopp *et al.*<sup>9</sup> Angle-integrated UPS measurements taken for a range of  $x$  values between 0 and 0.97 are then discussed in terms of the rigid-band model.

## II. EXPERIMENTAL RESULTS

Crystals of  $\text{Na}_x\text{WO}_3$  were prepared by the electrolysis of a melt of  $\text{Na}_2\text{WO}_4$  and  $\text{WO}_3$  with the use of the method described by Shanks.<sup>15</sup> The sodium concentrations of the crystals with  $x > 0.5$  were determined from the known relationship between the lattice constants and the  $x$  value, whereas the concentrations for  $x < 0.5$  were obtained directly from neutron-activation studies.

The measurements were carried out in a Vacuum Generator ADES 400 angle-resolved photoelectron spectrometer using Ne I (16.85 eV), He I (21.22 eV) and He II (40.8 eV) photons from a differentially pumped discharge lamp. The spectrometer was operated with energy and angle resolutions of 0.3 eV and  $3^\circ$ , respectively. Surface preparation was carried out in the vacuum chamber of the spectrometer which had a base pressure of  $\sim 2 \times 10^{-10}$  Torr.

Angle-resolved photoemission measurements were carried out on a cleaved (001) surface of  $\text{Na}_{0.85}\text{WO}_3$ . The low-energy electron diffraction (LEED) pattern of the surface was used to align the crystal. The geometry used for the angle-resolved measurements is shown in Fig. 2(a): The incoming photons and outgoing electrons lie in a plane normal to the crystal surface, and this plane can be rotated relative to the surface. The results presented here were taken for two fixed directions in the surface and as a function of the angle  $\theta$  between the photoemitted electrons and the surface normal. The photon incidence angle was held fixed at  $45^\circ$ .

It was not possible to obtain good cleaved single-crystal surfaces over the whole range of  $x$ , and a series of measurements was made on surfaces prepared using a diamond file. No angular dependence was found in the UPS spectra for any of these surfaces, the surface treatment apparently causing an angle averaging.

## III. RESULTS AND DISCUSSION

The investigation of the  $\text{Na}_x\text{WO}_3$  system was carried out in two parts. In the first part a detailed comparison of angle-resolved UPS (ARUPS) measurements with band-structure calculations was made for one sodium concentration. This comparison, which is described in Sec. III A below, revealed the presence of surface or defect states in addition to providing information about the effect of band-structure features on the spectra. Based on these results, an examination of the

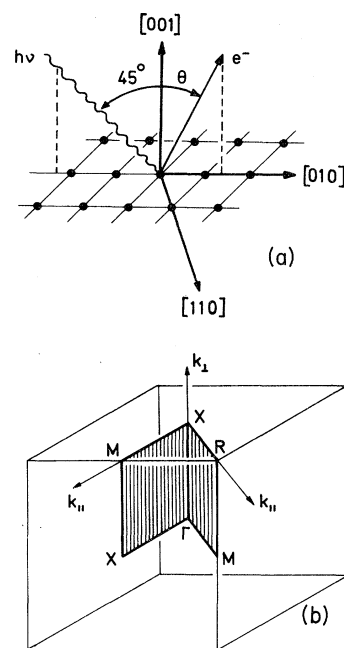


FIG. 2. (a) Geometrical arrangement for the ARUPS measurements and (b) the cubic Brillouin zone. Spectra were measured for the two electron emission directions shown in (a) and the initial-state wave vectors thus lie on the two shaded planes in the Brillouin zone.

composition-dependent trends in the spectra could be made. This second part of the investigation is described in Sec. III B.

### A. ARUPS measurements on $\text{Na}_{0.85}\text{WO}_3$

The uppermost three spectra in Fig. 3 are ARUPS measurements made at normal emission ( $\theta=0$ ) on the (001) surface of  $\text{Na}_{0.85}\text{WO}_3$ . An angle-integrated XPS spectrum is shown for comparison at the bottom of Fig. 3. The overall structure consisting of a conduction-band peak near the Fermi energy, a dip centered at 2 eV, and a broad valence-band peak is seen in all cases. This general behavior is predicted by all recent band-structure and density-of-states calculations for  $\text{Na}_x\text{WO}_3$  (Ref. 9) and related perovskite compounds (see Refs. 16 and 17, for example). More detailed comparisons must thus make use of the finer structure in the ARUPS data.

Experimental ARUPS data at low photon energies have been interpreted successfully in the direct model for the noble metals (see the review by Himpsel<sup>18</sup>), but for most materials, features arising from both direct and indirect transitions are seen

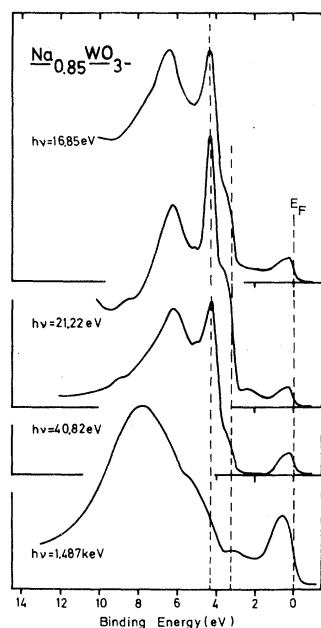


FIG. 3. Photoemission spectra of  $\text{Na}_{0.85}\text{WO}_3$ . The upper three spectra are ARUPS measurements made at normal emission and the bottom spectrum is from an XPS measurement.

in the ARUPS spectra.<sup>19</sup> For the results we show here, the indirect model seems appropriate because spectral features are seen in Fig. 3 to be independent of photon energy  $h\nu$ .

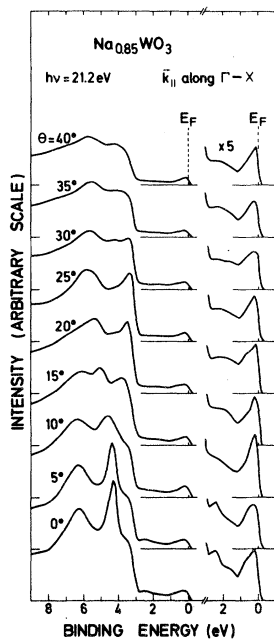


FIG. 4. ARUPS spectra of  $\text{Na}_{0.85}\text{WO}_3$  taken with 21.2-eV photons for  $\vec{k}_{\parallel}$  along  $\Gamma$ -X. Each spectrum is for a fixed value of the polar angle  $\theta$ .

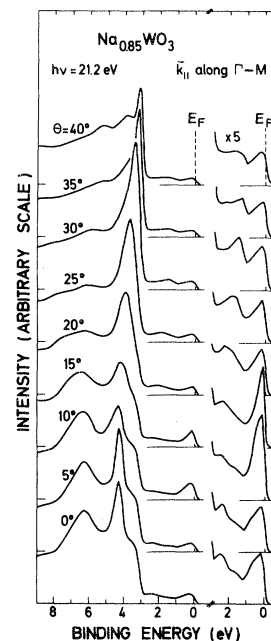


FIG. 5. ARUPS spectra of  $\text{Na}_{0.85}\text{WO}_3$  taken with 21.2-eV photons for  $\vec{k}_{\parallel}$  along  $\Gamma$ -M. Each spectrum is for a fixed value of the polar angle  $\theta$ .

The sharp peak at a binding energy of 4.3 eV in the three normal-emission spectra in Fig. 3 shows no energy dispersion as a function of  $h\nu$ . The shoulder at 3.25 eV and the broad peak at 6.3 eV also show virtually no photon energy dependence. The only features that vary with  $h\nu$  are a small peak which moves from 8.5 eV at  $h\nu=21.2$  eV to 9.0 eV at  $h\nu=40.8$  eV and a peak which appears in the gap between the valence and conduction bands in the  $h\nu=21.2$  eV spectrum. The former can be explained as a direct transition, but the latter is an extrinsic effect and will be discussed in more detail later.

Spectra for a range of polar angles  $\theta$  and for  $h\nu=21.2$  eV are given in Fig. 4 for emission in the plane of the surface normal and the [010] direction. For this geometry  $\vec{k}_{\parallel}$  is parallel to the direction  $\Gamma$ -X. Spectra for the same range of  $\theta$  are shown in Fig. 5 for the other symmetry direction of the surface, [110], for which  $\vec{k}_{\parallel}$  is parallel to  $\Gamma$ -M. It can be seen immediately that there are strong angle-dependent effects in the valence-band region and also in the conduction band and the "gap," the latter regions being shown on an expanded scale in Figs. 4 and 5. In order to make an exact comparison with theory,  $E(\vec{k})$  dispersions must be calculated along the vertical lines shown in the Brillouin zone in Fig. 2(b). Each of these lines corresponds to a fixed value of  $\vec{k}_{\parallel}$ , but only

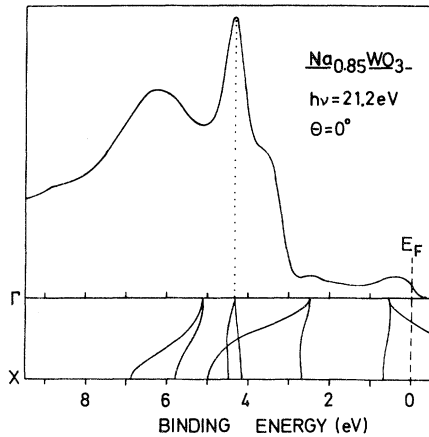


FIG. 6. Normal-emission ARUPS spectrum for  $\text{Na}_{0.85}\text{WO}_3$  compared with the band structure calculated along  $\Gamma$ - $X$  by Kopp *et al.* (Ref. 9) for  $\text{NaWO}_3$ .

three of them, viz.,  $\Gamma$ - $X$ ,  $X$ - $M$ , and  $M$ - $R$ , are directions for which band-structure calculations are normally given in the literature. As a first approximation we show a comparison of data for  $\vec{k}_{\parallel}$  along  $\Gamma$ - $X$  and  $\Gamma$ - $M$  with the band structure calculated by Kopp *et al.*<sup>9</sup> for  $\text{NaWO}_3$ .

The situation for normal emission is shown in Fig. 6. As mentioned earlier, the insensitivity of the spectra in Fig. 3 to variation of  $h\nu$  means that the ARUPS data can be thought of as representing the one-dimensional density of states in the band structure. The photoemission spectrum and the band structure have been aligned at the Fermi energy. One of the first things that can be seen is that the combined width of the valence and conduction bands is too small in the calculation. No matter which model of photoemission is used, the weak peak seen in the data near 8.5 eV cannot be explained by the band structure. The valence-band width and the band gap calculated by Kopp *et al.*<sup>9</sup> for  $\text{WO}_3$  have also been seen to be too small,<sup>13</sup> this shortcoming thus seeming to be a systematic failing of the calculation. It is likely that the shoulder near 8.5 eV arises from the lowest band in Fig. 6, requiring that the lowest two bands be moved downwards and stretched. If these two bands shift from 5.1 eV at  $\Gamma$  to about 6.5 eV, and the lower one is stretched so that it reaches  $X$  near 10 eV, then (i) the shoulder can be explained as a direct transition from the lower band (its energy was seen in Fig. 3 to depend on  $h\nu$ ), and (ii) the upper parts of the bands can contribute to the broad peak at 6.2 eV. The two bands that meet  $\Gamma$  at 2.5 eV must also be moved downward by 1 eV as the small peak in the gap region is not a bulk band-structure

effect. We are unable to tell from the data whether the two flat bands are correctly placed and give rise to the sharp peak seen in all the  $\theta=0$  measurements.

Comparison of the normal-emission ARUPS spectra with the band structure along  $\Gamma$ - $X$  has led us to conclude that the calculated position of the top of the valence band is too near the Fermi energy and that the valence-band width is too narrow. We can now make a similar comparison between the band structure along  $X$ - $M$  and the spectrum taken at  $\theta=25^\circ$  for  $\vec{k}_{\parallel}$  along  $\Gamma$ - $X$ . This comparison is not exact because for fixed  $\theta$  the length of  $\vec{k}_{\parallel}$  varies with binding energy, but for the valence-band region the variation is only  $\pm 10\%$ , and a useful comparison can still be made. The band structure and spectrum are shown in Fig. 7. As was the case for  $\Gamma$ - $X$ , the top of the valence band is too near the Fermi energy, by about 0.7 eV in this case. The large number of bands seen along this direction makes it almost impossible to make any detailed comparison of peak positions with particular bands, especially in view of the large shifts of bands which were seen to be necessary for  $\Gamma$ - $X$ .

If we now turn to an examination of the peak near the Fermi energy we also see discrepancies between the theory and the data. From the band structure we expect the photoemission peak to be much stronger for normal emission where there are two bands contributing to it than for the arrangement shown in Fig. 7 where there is only one band. Looking at the expanded region of Fig. 4, we can see that the peak heights are in fact very similar

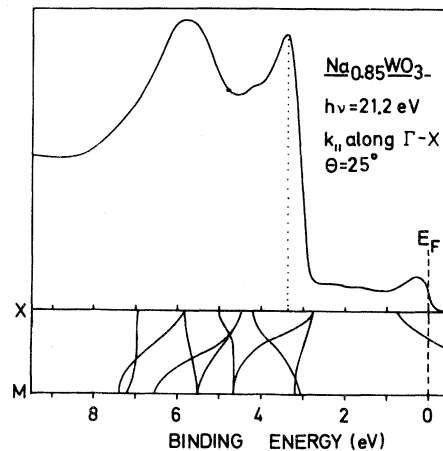


FIG. 7. ARUPS spectrum of  $\text{Na}_{0.85}\text{WO}_3$  for  $\vec{k}_{\parallel}$  along  $\Gamma$ - $X$  and for  $\theta=25^\circ$  compared with the band structure calculated along  $X$ - $M$  by Kopp *et al.* (Ref. 9) for  $\text{NaWO}_3$ .

for  $\theta=0$  and  $25^\circ$ . A more extreme example occurs for the direction  $MR$  in the Brillouin zone. The appropriate ARUPS spectrum, which is the  $\theta=35^\circ$  spectrum in Fig. 5, has a peak of similar intensity to the normal-emission curve. The band structure, however, has no band along  $M-R$  in this energy region.

It is unlikely that these discrepancies are due to an inadequacy of the band structure, because all other calculations for the perovskite group of materials (see Refs. 16 and 17 for example) give very similar conduction bands. Another alternative is that we are seeing the effect of an angle averaging due to the random distribution of sodium atoms, which should in turn lead to a breakdown of  $k$  conservation. A shoulder at 0.7 eV is also apparent for  $\theta \leq 25^\circ$  in both Figs. 4 and 5 and is possibly due to an angle averaging of a peak due to the second band along  $\Gamma-X$ . The much greater variation with the angle seen in the valence-band region is then a little surprising. A similar effect has been seen<sup>20</sup> in a study of the  $\text{Ge}(111)-(8)$  surface, which has a large number of small  $[\sim \frac{1}{8}\vec{G}(111)]$  surface reciprocal-lattice vectors. It was noted that angle averaging appeared to be a stronger effect in regions of the Brillouin zone in which gaps occur.

The third area of interest is the gap between the valence and conduction bands. It can be seen in Figs. 4 and 5 that there is structure in this region which has the same order of magnitude as the conduction-band peak. In previous XPS (Refs. 10, 21, and 22) and UPS (Ref. 23) investigations a peak in this region was noted and assigned to a plasmon loss associated with the conduction band.<sup>10,21,22</sup> Electron-energy-loss studies<sup>24,25</sup> and optical measurements<sup>26-28</sup> do indeed show a sharp peak in the energy-loss function between 2.0 and 2.5 eV, which is due to plasma oscillation of the conduction electrons. A plasmon peak with this energy is also seen in XPS core line measurements.<sup>10,21,22</sup> The comparison with the ARUPS data shows that the interpretation of the XPS peak as a plasmon is quite possibly incorrect. In Fig. 3 we show the XPS spectrum for  $\text{Na}_{0.85}\text{WO}_3$  and compare it with the normal-emission ARUPS data. The peak in question at  $\sim 3$  eV in the XPS spectrum can be seen to be close to one of the valence-band features and is certainly not in the gap region. If we look at Fig. 5, which shows the data for  $\vec{k}_{\parallel}$  along  $\Gamma-M$ , the high-angle spectra have a very strong peak at 3.2 eV. It is quite likely then, that the peak in the (angle-integrated) XPS spectrum is in fact due to a peak in the valence band.

We cannot completely rule out the plasmon theory for XPS because the photon-energy dependence of the photoionization cross section makes the XPS experiment much more sensitive to  $d$  states than to the oxygen  $p$  states near the top of the valence band. This effect has been discussed previously for  $\text{WO}_3$  (Ref. 13) with the use of partial density-of-states calculations of Kopp *et al.*<sup>9</sup>

In the ARUPS case, the peak in the gap region cannot be due to plasmon excitation because its energy separation from the conduction-band peak is always less than 2.1 eV, becoming as small as 1.2 eV at high angles. The energy-loss data, on the other hand, shows the surface plasmon to have an energy of 2.0 eV for  $\text{Na}_{0.85}\text{WO}_3$  (Ref. 24), and the optical results give the bulk plasmon energy as 2.3 eV for this composition.<sup>27,28</sup> We can also rule out the possibility that the gap peak is due to  $\text{He I}^*$  satellite radiation because the peak is also present in the  $\text{He II}$  and  $\text{Ne I}$  spectra in Fig. 3.

One of the most likely possibilities is that the peak in the gap region is a surface state. As can be seen from Fig. 1, the (001) surface of  $\text{Na}_x\text{WO}_3$  must have a composition of  $\text{WO}_2$  or  $\text{Na}_x\text{O}$  (or domains of both) after cleaving. In either case the surface atoms are not fully coordinated and the surface electronic structure would not be expected to be the same as that in the bulk. Theoretical investigations have shown that surface states can exist in the region above the top of the valence band for similar materials. Ellialtioglu and Wolfram<sup>29</sup> have examined the electronic structure of the transition-metal perovskites and calculated the local density of states for the transition-metal atom when it is fully coordinated and when it has one oxygen atom missing. The latter situation occurs at the (001) surface of  $\text{Na}_x\text{WO}_3$  with the  $\text{WO}_2$  composition. Ellialtioglu and Wolfram found that surface states appeared in the bulk band gap for the insulating transition-metal perovskites such as  $\text{SrTiO}_3$  if Coulomb effects were ignored. These states were pushed above the Fermi energy, however, when the Coulomb effects were taken into account. The final conclusion that no occupied surface states existed in the bulk band gap agreed with earlier photoemission measurements of  $\text{SrTiO}_3$ .<sup>30</sup> It was also predicted that oxygen vacancies near the surface would stabilize surface states in the gap, again in agreement with experimental results for  $\text{TiO}_2$  (Ref. 31) and  $\text{SrTiO}_3$  (Ref. 30). Although they did not make the calculation explicitly, Ellialtioglu and Wolfram<sup>29</sup> suggested that the screening effect of conduction electrons could also stabilize the surface states in the gap region. Con-

duction electrons are indeed present for metallic  $\text{Na}_x\text{WO}_3$ , and so the peak we see in the gap region of  $\text{Na}_{0.85}\text{WO}_3$  is quite possibly a surface state.

Further evidence for this conclusion comes from both theoretical and experimental results. Ellialtioglu and Wolfram<sup>29</sup> calculated the dispersion of the surface state and found, in agreement with what we see in Figs. 4 and 5, that the state disperses upwards away from  $\Gamma$ . UPS experiments carried out on the (001) surface of  $\text{WO}_3$  have shown the presence of states in this region for surfaces which were argon ion bombarded and annealed.<sup>13</sup> The  $\text{WO}_3$  surface when treated this way has a considerable density of conduction electrons, as revealed by a peak at the Fermi energy in the UPS spectrum, which can provide the screening required in the model of Ellialtioglu and Wolfram.<sup>29</sup> That the peak near 2 eV is associated with a surface effect, is also suggested by the variation in its intensity for different cleaves.

It should be pointed out that Langell and Bernasek<sup>32</sup> have concluded from the results of their Auger and low-energy electron diffraction (LEED) experiments that one half of the surface unit cells contain a sodium atom for  $\text{Na}_{0.8}\text{WO}_3$ . The surfaces which they examined were not cleaved but annealed in an oxygen partial pressure environment, and thus it is possible that we are looking at a completely different surface structure. Nevertheless, it is not certain whether or not the surface tungsten atoms are fully coordinated in the annealed surface, so it is possible that the results of Langell and Bernasek are consistent with the existence of a surface state. There have also been suggestions of a depletion of sodium from the surface region of the sodium bronzes.<sup>10</sup> Recent Auger measurements by Weber *et al.*,<sup>33</sup> however, have not indicated any sodium depletion at the surface. An analysis of XPS core line intensities<sup>12</sup> has also shown no evidence of sodium depletion.

#### B. $x$ -dependent electronic structure

Results of UPS measurements made on samples of different composition are shown in Fig. 8. Measurements were made at normal emission with the ARUPS spectrometer used for the angle-dependent measurements described in the preceding section. Clean surfaces of  $\text{Na}_x\text{WO}_3$  were prepared using a diamond file in the vacuum. The method used to clean the  $\text{WO}_3$  surface has been described in detail elsewhere.<sup>13</sup> As a result of these treatments, the spectra showed no dependence on the

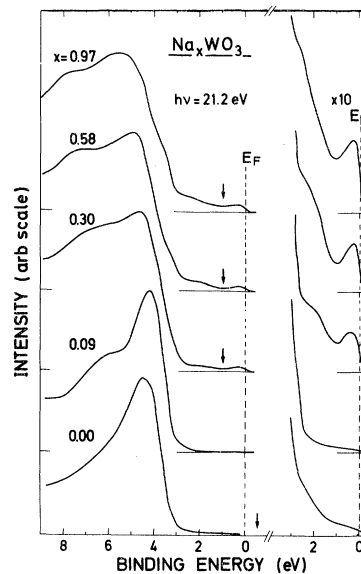


FIG. 8. UPS spectra for  $\text{Na}_x\text{WO}_3$  for a range of values of  $x$ . The spectra are aligned at the Fermi energy and the position of the bottom of the conduction band is shown by the arrows.

emission angle, indicating that the curves in Fig. 8 represent an integrated density of states.

The upper three spectra in Fig. 8 are for metallic samples and have been aligned at the Fermi energy. These spectra can be broken up into three regions: (i) the conduction band, which extends from the Fermi energy to a binding energy of 1.0 eV, (ii) the "gap" region between 1.0 and about 3.0 eV, and (iii) the valence band at binding energies greater than 3 eV. If the rigid-band model is appropriate for metallic  $\text{Na}_x\text{WO}_3$  and if we use the density of states from Kopp *et al.*,<sup>9</sup> we would expect the Fermi energy to move by about 0.7 eV relative to all spectral features as  $x$  increases from 0.30 to 0.97. Although we find that the two broad features at 4.6 and 7.0 eV in the valence band of the  $x=0.30$  sample move by roughly the predicted amount, all the other trends do not favor a rigid-band model.

The top of the valence band remains at about 3.0 eV for all three spectra and, more strikingly, the width of the occupied part of the conduction band is completely independent of  $x$  in the metallic region.

It should be mentioned that Egdal and Hill,<sup>34</sup> who recently reported on weak  $x$ -dependent features in the conduction-band peak of their photoemission data, did their measurements on high-temperature-annealed powdered samples. We found that annealing above 550°C is enough to

produce extra structure in the conduction band of our cleaved samples, which is probably related to a small amount of oxygen deficit at the surface.

The position of the bottom of the conduction band occurs at the dip near 1 eV in the spectra for metallic samples, and is shown by the arrows in Fig. 8. The fact that the bottom of the conduction band remains fixed relative to the Fermi energy is strong evidence that a rigid conduction band is not being filled as  $x$  increases. An alternative explanation that the density of conduction-band states increases with  $x$  seems to fit the data better. This alternative is also consistent with the  $x$ -dependent behavior of the specific-heat coefficient and the magnetic susceptibility. Both of these quantities vary linearly with  $x$  for cubic  $\text{Na}_x\text{WO}_3$  crystals with values of  $x > 0.22$ .<sup>14</sup> In Fig. 9 we show a plot of the electronic specific-heat coefficient from the paper by Zumsteg,<sup>14</sup> which also includes data from Vest *et al.*<sup>35</sup>

The coefficient  $\gamma$  is simply related to the density of states at the Fermi energy,  $N(E_F)$ , by

$$\gamma = \frac{1}{3} \pi^2 k_B^2 N(E_F),$$

where  $k_B$  is Boltzmann's constant. The dashed line in Fig. 9 shows the expected  $x^{1/3}$  behavior for a free-electron conduction band in the rigid-band model. The  $x$  dependence expected for  $\gamma$  on the basis of the density of states of Kopp *et al.*<sup>9</sup> is shown by the solid line, and the dotted line shows the dependence expected from a nearly free electron band with  $m^* = 1.83m_0$ . It is clear that the heat-capacity data do not fit a nearly-free-electron rigid-band model.

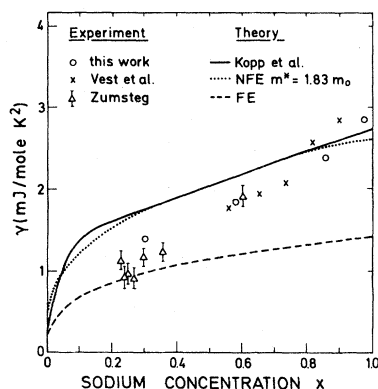


FIG. 9. Electronic specific-heat coefficient  $\gamma$  as a function of  $x$  after Zumsteg (Ref. 14). The dashed and dotted lines show the behavior expected from a free-electron theory with  $m^* = m_0$  and  $m^* = 1.83m_0$ , respectively. The solid line is the behavior expected from the DOS calculation of Kopp *et al.* (Ref. 9).

Values of  $N(E_F)$  from the UPS results are also plotted in Fig. 9 as circles, normalized to the electronic specific-heat coefficient at  $x=0.60$ . The  $x$ -dependent behavior for  $N(E_F)$  is similar, and both our UPS results and the specific-heat results fit a model in which  $N(E_F)$  increases linearly with  $x$ . It should be pointed out here that a linear increase of  $N(E_F)$  with  $x$  has also been concluded by Greiner *et al.*<sup>36</sup> from magnetic-susceptibility measurements and recently by Egdell and Hill<sup>34</sup> from angle-integrated UPS. Kamitakahara *et al.*<sup>37</sup> interpreted their finding of a concentration-dependent Kohn anomaly in  $\text{Na}_x\text{WO}_3$  in terms of a rigid-band model but their results are also consistent with a linear increase in the conduction-band density of states (CBDOS).

Further evidence against the rigid-band model is provided by the fact that the valence-band shape is not independent of  $x$  in the metallic region. Compared to the  $x=0.30$  spectrum, a new shoulder appears near the top of the valence band for the  $x=0.58$  sample and increases in intensity for  $x=0.97$ . The conclusion that the rigid-band model is inappropriate for metallic  $\text{Na}_x\text{WO}_3$  is in agreement with the findings of our earlier XPS investigation.<sup>11</sup>

In the gap region of the metallic materials, the density of states increases with  $x$  and the position of the shoulder moves away from the conduction band. These efforts are consistent with the model of Ellialtioglu and Wolfram,<sup>29</sup> which was discussed in the preceding section. In the model, decreasing screening causes surface states in this region to be pushed towards the conduction band. Figure 8 shows that there are no states in the gap region for the nonmetallic spectra, again in agreement with the model.

Spectra for the nonmetallic compounds  $\text{WO}_3$  and  $\text{Na}_{0.09}\text{WO}_3$  are shown in the lower part of Fig. 8. The valence-band region of the  $\text{WO}_3$  spectrum differs from those of the sodium bronzes in that it only has one valence-band peak, whereas the bronzes all have two main features. In an earlier paper that described photoemission results for  $\text{WO}_3$  (Ref. 13), it was shown that the Fermi energy is fixed at 0.5 eV below the bottom of the conduction band on the clean surface. In the bulk the Fermi energy is within 0.04 eV of the conduction band,<sup>38</sup> but band bending alters this situation at the surface. To enable comparison with the metallic samples, the onset of the conduction band is shown in Fig. 8 by arrows. It can be seen immediately that the separation between the top of the valence band and the bottom of the conduction band is



greater by about 1.7 eV for  $\text{WO}_3$  than for  $\text{Na}_{0.30}\text{WO}_3$ . The band-structure calculations of Kopp *et al.*,<sup>9</sup> which showed that  $\text{WO}_3$  has a band gap of 1.55 eV and  $\text{NaWO}_3$  has a separation between valence and conduction bands of 1.75 eV are thus considerably in error in this energy region.

It is more difficult to make a comparison with the  $\text{Na}_{0.09}\text{WO}_3$  spectrum as the position of the conduction band is not certain. If the extra electrons associated with the sodium atoms are localized near the conduction band, then it should be possible to see them with UPS measurements. The analogy with  $\text{WO}_3$  suggests that the failure to see the states near the top of the gap may be the result of a band-bending effect. If the bands bend upward towards the surface as in Fig. 10 then the localized states can be emptied near the surface. We must now examine whether an effect such as this is possible for  $\text{Na}_{0.09}\text{WO}_3$  and whether it is consistent with the other features in the UPS spectrum.

The required charge separation at the surface can occur if the surface has the  $\text{Na}_x\text{O}$  composition. Oxygen atoms on the surface are acceptors and can accumulate up to one electron, leaving fixed positive charges in the bulk. The maximum depth  $z_0$  of the depletion layer occurs when there is one electron per surface oxygen and is thus 30 Å for  $\text{Na}_{0.09}\text{WO}_3$ . For a surface layer of negative charge and a uniform density of fixed positive charges, the band bending is given by<sup>39</sup>

$$V(\text{bulk}) - V(z) = \frac{1}{2}eN_D(z - z_0)^2/\epsilon\epsilon_0,$$

where  $N_D$  is the volume density of donor atoms,  $z$  is the distance from the surface, and  $\epsilon$  is the static dielectric constant of the solid. Substituting the sodium density in  $\text{Na}_{0.09}\text{WO}_3$  for  $N_D$ ,  $z_0 = 30$  Å, and the static dielectric constant  $\epsilon \sim 1000$  for  $\text{WO}_3$ ,<sup>40</sup> a band bending of the order of 1 eV is possible.

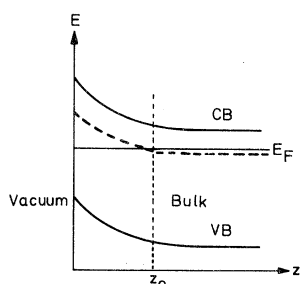


FIG. 10. Band bending for  $\text{Na}_{0.09}\text{WO}_3$  which causes the localized states (dashed line) to be emptied at the surface.

The bottom of the conduction band could thus reasonably be placed at about 0.75 eV above the Fermi energy so that the valence-band peaks for  $\text{WO}_3$  and  $\text{Na}_{0.9}\text{WO}_3$  are aligned and so that the localized states near the conduction band are emptied at the surface. One difficulty with this model is that the valence-band edge in the  $\text{Na}_{0.09}\text{WO}_3$  spectrum in Fig. 8 is rather sharp, implying that the depth ( $\sim 10$  Å) probed by the UPS measurement does not have large band curvature. If the band bending penetrates the maximum amount of  $\sim 30$  Å we require that all tungsten atoms are fully coordinated with oxygen atoms, in contradiction to the surface of the metallic compounds where we assumed that at least some of the surface has the  $\text{WO}_2$  composition. Although a band-bending effect provides a reasonable explanation of why localized states are not seen, it must be regarded as tentative until experiments are carried out which explicitly test whether the bands bend.

Regardless of how far the conduction-band edge is above the Fermi energy in the  $x=0.09$  sample, the following conclusions can be made from the spectra in Fig. 8.

- (i) The valence-band density of states changes shape continuously as a function of  $x$ .
- (ii) The size of the gap between the valence and conduction band remains roughly constant at about 2 eV for the metallic materials, is at least as large as 3.2 eV for  $x=0.09$ , and is around 3.5 eV for  $\text{WO}_3$ .
- (iii) States that have been assigned to surface states occur in the gap region for the metallic material, increasing in intensity as  $x$  increases, but are absent for  $x=0.09$  and  $x=0$ .

(iv) Conduction-band states are seen for the metallic materials, but their band width does not increase as expected for a rigid-band model.

From the UPS spectra one can determine the work function  $\phi$  for these materials and the values obtained are shown in Fig. 11. The work function shows an overall decrease as  $x$  increases. Values reported earlier by Chambers and Swanson<sup>41</sup> for two metallic samples of  $\text{Na}_x\text{WO}_3$  agree with our data. We will not discuss in detail the values for the nonmetallic samples because the effects of band bending complicate the interpretation. The very high value of  $\phi$  for  $x=0.09$  is, however, supportive evidence for band bending at this composition.

The linear decrease of  $\phi$  with increasing sodium concentration, seen for the metallic samples, is typical for an alloy in which there is no surface enrichment of one of the constituents.<sup>42</sup> The linearity seen in Fig. 11 also shows that there are no

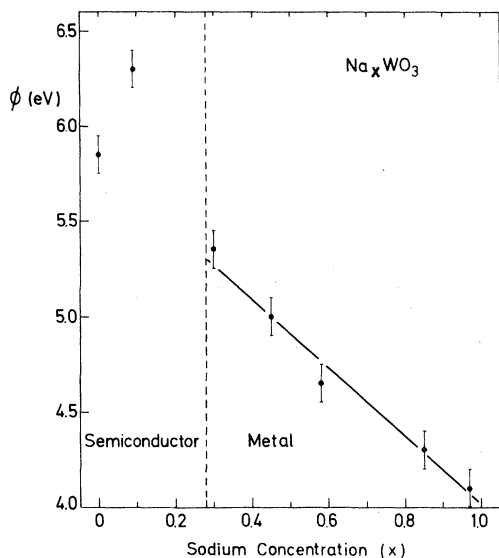


FIG. 11. Work function  $\phi$  for  $\text{Na}_x\text{WO}_3$  determined from the UPS spectra shown as a function of the sodium concentration.

abrupt changes in the surface composition between  $x=0.3$  and 1.0. For their annealed samples of  $\text{Na}_x\text{WO}_3$ , Langell and Bernasek<sup>32</sup> claim that the surface layer has a sodium concentration that does not vary linearly with the bulk concentration. Our results for filed samples do not agree with this model.

#### IV. CONCLUSIONS

The results obtained by angle-resolved and angle-integrated ultraviolet photoemission spectroscopy carried out over the entire sodium concentration range in the sodium-tungsten-bronze system can be summarized as follows.

For the metallic samples of  $\text{Na}_x\text{WO}_3$  with

$x > 0.3$ , the top of the valence band and the bottom of the conduction band remain at 3 eV and 1 eV respectively. The width of the conduction-band peak is 0.8 eV and is independent of  $x$ . This result and the observed linear dependence of the peak intensity at the Fermi level with increasing  $x$ , are strong indications that the rigid-band model fails to explain the observed behavior in the metallic region of the sodium-tungsten-bronze system. These UPS results corroborate the interpretation of our earlier XPS measurements of the same system.<sup>11</sup>

A peak in the gap is observed for metallic samples, and for  $\text{Na}_{0.85}\text{WO}_3$  it exhibits a dispersion from 2.1 eV for  $k_{\parallel}=0$  to 1.2 eV for  $\vec{k}_{\parallel}$  along  $\Gamma$ - $M$ . Following the suggestions made by Ellialtioglu and Wolfram<sup>29</sup> about the position of a localized surface state in transition-metal perovskites, it is most likely that the observed peak in the gap originates from surface states.

The failure to detect localized gap states for the semiconducting samples can be explained by band-bending effects originating from oxygen acceptor states at the surface. A charge depletion layer with a thickness of about 30 Å can occur when free electrons from bulk sodium atoms accumulate at surface oxygen atoms.

The observed linear decrease of the work function  $\phi$  with increasing  $x$  indicates that there is no segregation or sodium depletion near the surface as it was suggested in earlier investigations.<sup>10,32</sup>

#### ACKNOWLEDGMENTS

One of us (R.D.B.) would like to thank the Alexander von Humboldt Foundation for financial support. Ames Laboratory is operated for the U.S. Department of Energy by Iowa State University under Contract No. W-7405-Eng-82. This work was supported in part by the Director for Experimental Research, Office of Basic Material Science.

\*Present address: Stanford Synchrotron Radiation Laboratory, Stanford University, Stanford, CA 94305.

<sup>1</sup>P. A. Lightsey, Phys. Rev. B **8**, 3586 (1973).

<sup>2</sup>I. Webman, J. Jortner, and M. H. Cohen, Phys. Rev. B **13**, 713 (1976).

<sup>3</sup>D. P. Tunstall, Phys. Rev. B **14**, 4735 (1976).

<sup>4</sup>N. F. Mott, Philos. Mag. **35**, 111 (1977).

<sup>5</sup>D. P. Tunstall and W. Ramage, J. Phys. C **13**, 725 (1980).

<sup>6</sup>D. P. Tunstall, Phys. Rev. B **11**, 2821 (1975).

<sup>7</sup>P. A. Lightsey, D. A. Lilienfeld, and D. F. Holcomb, Phys. Rev. B **14**, 4730 (1976).

<sup>8</sup>R. Clarke, Phys. Rev. Lett. **39**, 1550 (1977).

<sup>9</sup>L. Kopp, B. N. Harmon, and S. H. Liu, Solid State Commun. **22**, 677 (1977).

<sup>10</sup>J.-N. Chazalviel, M. Campagna, G. K. Wertheim, and H. R. Shanks, Phys. Rev. B **16**, 697 (1977).

<sup>11</sup>G. K. Wertheim and J. N. Chazalviel, Solid State Commun. **40**, 931 (1981).

<sup>12</sup>H. Höchst, R. D. Bringans, H. R. Shanks, and P.

- Steiner, *Solid State Commun.* **37**, 41 (1980).
- <sup>13</sup>R. D. Bringans, H. Höchst, and H. R. Shanks, *Phys. Rev. B* **24**, 3481 (1981).
- <sup>14</sup>F. C. Zumsteg, *Phys. Rev. B* **14**, 1406 (1976).
- <sup>15</sup>H. R. Shanks, *J. Cryst. Growth* **13/14**, 433 (1972).
- <sup>16</sup>L. F. Mattheiss, *Phys. Rev.* **181**, 987 (1969).
- <sup>17</sup>T. Wolfram and S. Ellialtioglu, in *Theory of Chemisorption*, edited by J. R. Smith (Springer, Heidelberg, 1980), p. 149.
- <sup>18</sup>F. J. Himpsel, *Appl. Opt.* **19**, 3964 (1980).
- <sup>19</sup>T. Grandke, L. Ley, and M. Cardona, *Phys. Rev. B* **18**, 3847 (1978).
- <sup>20</sup>R. D. Bringans and H. Höchst, *Phys. Rev. B* **25**, 1081 (1982).
- <sup>21</sup>M. Campagna, G. K. Wertheim, H. R. Shanks, F. Zumsteg, and E. Banks, *Phys. Rev. Lett.* **34**, 738 (1975).
- <sup>22</sup>G. K. Wertheim, M. Campagna, J.-N. Chazalviel, and D. N. E. Buchanan, *Appl. Phys.* **13**, 225 (1977).
- <sup>23</sup>R. L. Benbow and Z. Hurych, *Phys. Rev. B* **17**, 4527 (1978).
- <sup>24</sup>R. E. Dietz, M. Campagna, J.-N. Chazalviel, and H. R. Shanks, *Phys. Rev. B* **17**, 3790 (1978).
- <sup>25</sup>M. A. Langell and S. L. Bernasek, *Phys. Rev. B* **23**, 1584 (1981).
- <sup>26</sup>D. W. Lynch, R. Rosei, J. H. Weaver, and C. G. Olson, *J. Solid State Chem.* **8**, 242 (1973).
- <sup>27</sup>P. Campagni, A. Manara, G. Campagnoli, A. Gustinetti, and A. Stella, *Phys. Rev. B* **15**, 4623 (1977).
- <sup>28</sup>J. F. Owen, K. J. Teegarden, and H. R. Shanks, *Phys. Rev. B* **18**, 3827 (1978).
- <sup>29</sup>S. Ellialtioglu and T. Wolfram, *Phys. Rev. B* **18**, 4509 (1978).
- <sup>30</sup>V. E. Henrich, G. Dresselhaus, and H. J. Zeiger, *Phys. Rev. B* **17**, 4908 (1978).
- <sup>31</sup>V. E. Henrich, G. Dresselhaus, and H. J. Zeiger, *Phys. Rev. Lett.* **36**, 1335 (1976).
- <sup>32</sup>M. A. Langell and S. L. Bernasek, *J. Vac. Sci. Technol.* **17**, 1287 (1980).
- <sup>33</sup>M. F. Weber, H. R. Shanks, A. J. Bevelo, and G. C. Danielson, *J. Electrochem. Soc.* **127**, 329 (1980).
- <sup>34</sup>R. G. Egdell and M. D. Hill, *Chem. Phys. Lett.* **85**, 140 (1982).
- <sup>35</sup>R. W. Vest, M. Griffel, and J. F. Smith, *J. Chem. Phys.* **28**, 293 (1958).
- <sup>36</sup>J. D. Greiner, H. R. Shanks, and J. F. Smith, *J. Chem. Phys.* **28**, 272 (1962).
- <sup>37</sup>W. A. Kamitakahara, B. N. Harmon, J. G. Taylor, L. Kopp, H. R. Shanks, and J. Rath, *Phys. Rev. Lett.* **36**, 1393 (1976).
- <sup>38</sup>J. M. Berak and M. J. Sienko, *J. Solid State Chem.* **2**, 109 (1970).
- <sup>39</sup>S. R. Morrison, *The Chemical Physics of Surfaces* (Plenum, New York, 1977).
- <sup>40</sup>B. L. Crowder and M. J. Sienko, *J. Chem. Phys.* **38**, 1576 (1963).
- <sup>41</sup>S. A. Chambers and L. W. Swanson, *Appl. Surf. Sci.* **4**, 82 (1980).
- <sup>42</sup>J. Hölzl and F. K. Schulte, in *Solid Surface Physics* Vol. 85 of *Springer Tracts in Modern Physics*, edited by G. Höhler (Springer, Berlin, 1979).